Thermophysics and Aeromechanics, *2004*, *Vol. 11*, *No. 3*

NONLINEAR SINUSOIDAL AND VARICOSE INSTABILITY IN THE BOUNDARY LAYER (REVIEW)*

Yu.A. LITVINENKO[1], V.G. CHERNORAY[1], V.V. KOZLOV[1], L. LOEFDAHL[2], G.R. GREK[1], and H. CHUN[3]

[1]*Institute of theoretical and Applied Mechanics SB RAS*, *Novosibirsk*, *Russia*

[2]*Chalmers University of Technology*, *Goeteborg*, *Sweden*

[3]*Pusan National University*, *Pusan*, *South Korea*

(*Received May 27*, *2004*)

Results of studying sinusoidal and varicose instabilities of streaky structures at the nonlinear stage of the laminar-turbulent process in shear flows are presented. The flow behavior in the course of spatial evolution of streaky structures with a secondary high-frequency disturbance generated on them is discussed. Various scenarios of origination and development of coherent vortex structures examined in physical and numerical experiments are considered. Specific features of the development of sinusoidal and varicose cases of destruction of the steady streamwise streaky structure are demonstrated, such as transverse and streamwise modulation of the structure by the secondary-disturbance frequency, appearance of new streaky structures in the downstream direction, and emergence and evolution of unsteady Λ-type structures localized in space in both cases.

INTRODUCTION

It is known [Kachanov, 1982] that the laminar-turbulent transition in the case of low degree of free-stream turbulence is associated with origination and development of instability waves (the so-called Tollmien —Schlichting waves). In their downstream evolution, these waves can grow linearly at first, then they experience the nonlinear stage of development, and finally lead to flow turbulization. The linear stage of development of instability waves has been studied in sufficient detail both theoretically and experimentally, but the nonlinear stage and especially its last stages have not been adequately examined. The most important results in these studies have been achieved in physical and numerical experiments. The two-dimensional Tollmien — Schlichting wave at the nonlinear stage of its evolution reaches a certain amplitude (Fig. 1) and suffers a three-dimensional distortion, which results in emergence of typical three-dimensional Λ-structures [Klebanoff, 1962; Saric, 1984; Kachanov, 2003].

The specific feature of origination and development of these structures is the fact that they are not only typical of the classical laminar-turbulent transition [Klebanoff, 1962], but also are a mandatory attribute of the transition in more complicated flows, such as the flows modulated by streamwise streaky structures of the Goertler-vortex type (Figs. 2 and 3) [Floryan, 1991; Bippes, 1972; Ito, 1985], crossflow vortices on swept wings,

* This work was supported by the Russian Foundation for Basic Research (Grant No. 02-01-00006), by the President of the Russian Federation (Grant No. NSh-964.2003.1), and by INTAS (Grant No. 00-00232).

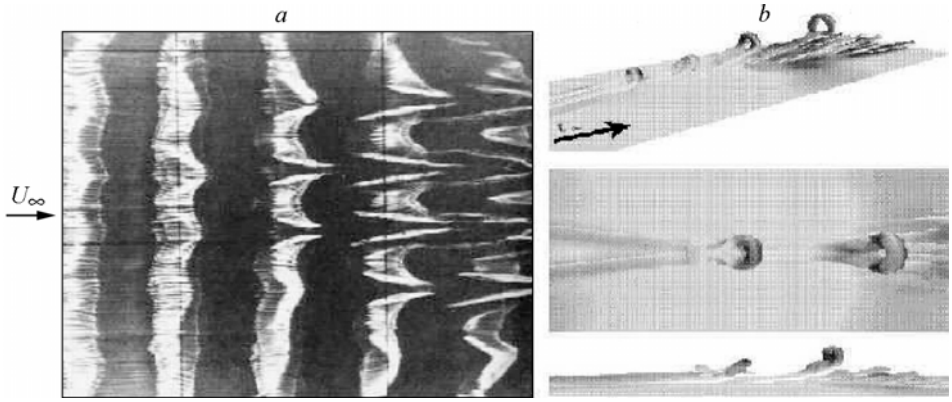

Fig. 1. Visualization of formation of Λ-structures (*a*) (from [Saric, 1984]) and numerical simulation of Kachanov's experiment by U. Rist (*b*) (from [Kachanov, 2003]).

etc., and also in the viscous sublayer of the turbulent boundary layer. In these situations, they arise, in particular, because of the secondary high-frequency instability of such flows and can be manifested not only as Λ-structures but also in the form of horse-shoe (Ω-structures), hairpin, and other vortices. Nevertheless, the common feature of these structures is the presence of two counterrotating vortices (legs of the structure) coupled by the "head". It is the dynamics of downstream development of these structures that is the reason for flow turbulization in many cases. A typical feature of evolution of these structures, e.g., on a swept wing is the disappearance of one counterrotating vortex because of the crossflow, whereas the classical Λ–structure is developed on a nonswept wing [Pratt, 2001]. Figure 4 shows the three-dimensional patterns of development of Λ-structures on nonswept and swept wings, which were obtained by hot-wire measurements [Pratt, 2001]. At a slip angle of 30°, the Λ-structures become asymmetric; at 45°, only one out of two counterrotating vortices is left.

The mechanism of origination and evolution of these structures has been studied in numerous experimental [Boiko, 2002; Panton, 2001; Acarlar, 1987; Haidary, 1994; Grek, 2000] and numerical [Rist, 1998; Renter, 2000; Zhou, 1999] researches. It was shown in these studies that the mechanism of turbulence generation in various near-wall

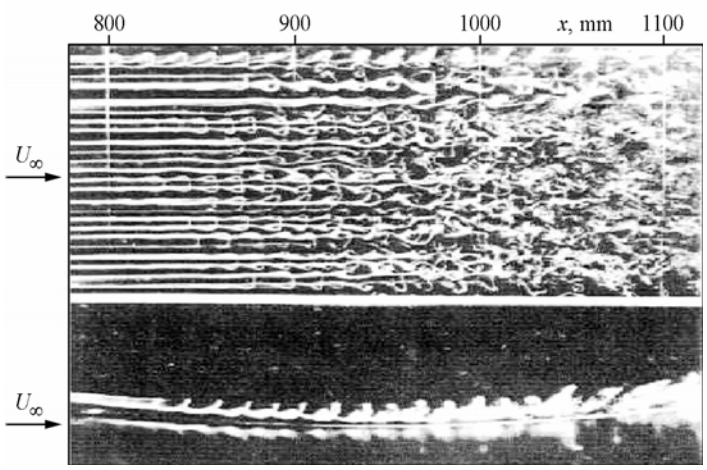

Fig. 2. Formation of horse-shoe structures on Goertler vortices — varicose instability (from [Floryan, 1991] and [Ito, 1985]).

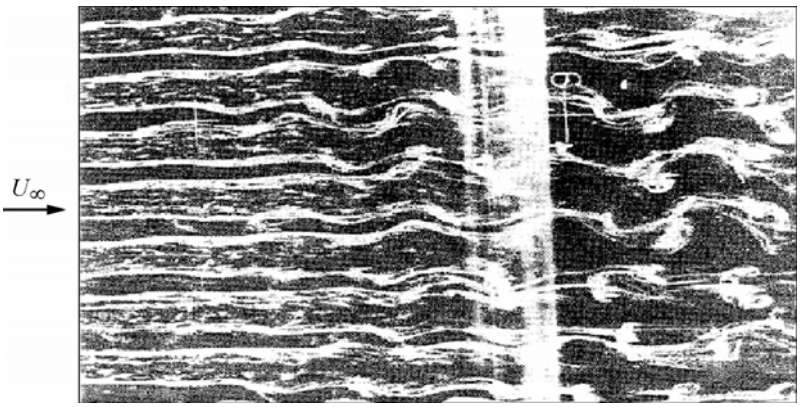

Fig. 3. Secondary instability of Goertler vortices of the sinusoidal type (from [Floryan, 1991] and [Bippes, 1972]).

transitional (e.g., harmonic and subharmonic types of the classical transition) and turbulent flows is identical and is associated with origination, development, and destruction of coherent structures, such as Λ-structures, Ω-structures, etc.

On the other hand, as was mentioned above, the initial instability of many flows is related to their transverse modulation by steady (Goertler vortices, crossflow vortices on swept wings, etc.) and unsteady streamwise structures (streaky structures in the case of elevated free-stream turbulence, Λ-, Ω-, and hairpin vortices, etc.). Transverse modulation of flows by these structures generates conditions (unstable inflectional profiles of velocity normal to the surface $\partial U/\partial y$ and across the flow $\partial U/\partial z$) for origination and development of secondary high-frequency oscillations whose downstream evolution leads to boundary-layer turbulization. The streaky structures have been also found in the viscous sublayer of the turbulent boundary layer about 50 years ago (Fig. 5), and their role in the mechanism of regeneration of turbulent oscillations by means of downstream evolution of streaky structures has been examined experimentally, analytically, and numerically since that time. The destruction of streaky structures in the downstream direction with formation of typical vortex structures is clearly seen in Fig. 6.

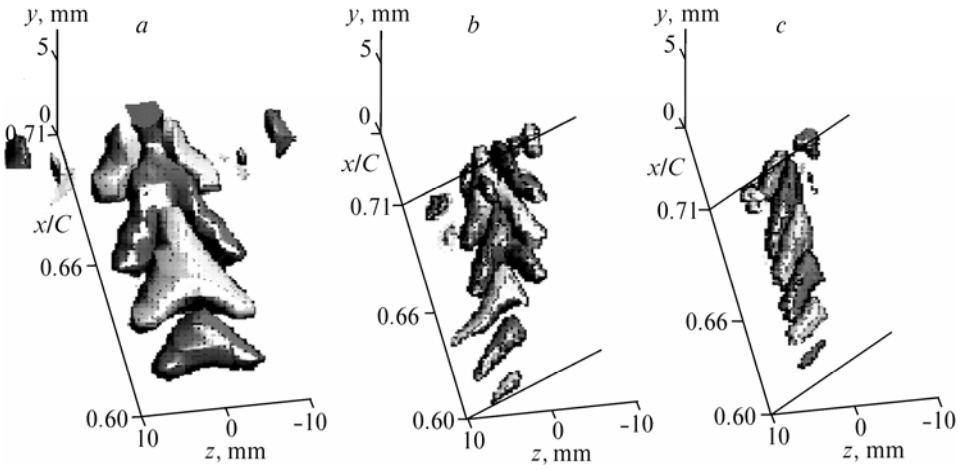

Fig. 4. Development of Λ-structures on a nonswept (*a*) and swept wing with a slip angle of 30° (*b*) and 45° (*c*) (spatial patterns of disturbance evolution are borrowed from[Pratt, 2001]).

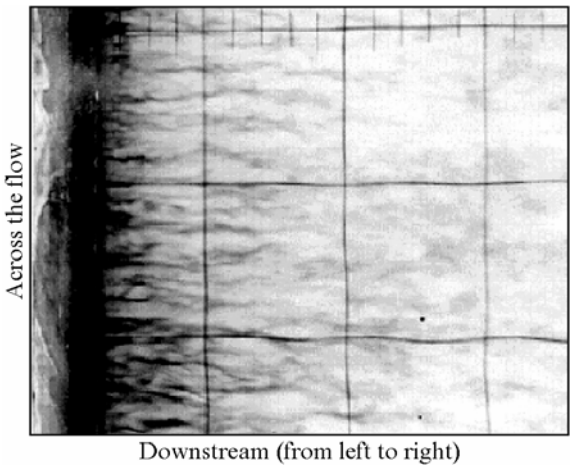

Fig. 5. Visualization of the flow in a viscous sublayer of a turbulent boundary layer ((F. Hama) from [Panton, 2001]).

The results of direct numerical simulation of coherent structures in a turbulent flow in a channel are shown in Fig. 7, a. Typical Λ-structures are clearly visible. The flow structure in the viscous sublayer of the turbulent boundary layer is shown in Fig. 7, b. The authors identify different types of coherent structures arising in the viscous sublayer.An important aspect of coherent structures is their role in turbulization of free jet flows. As was shown in [Kozlov, 2002; Litvinenko, Kozlov, 2004], the streaky structures appear in circular or plane jets directly at the nozzle exit. In the case of interaction of two-dimensional Kelvin — Helmholtz vortex rings with streaky structures, their three-dimensional distortion occurs with formation of typical azimuthal spikes in the form of Λ- or Ω-shaped structures (Fig. 8). The scenario of this process resembles the three-dimensional distortion of the classical two-dimensional Tollmien — Schlichting wave at the nonlinear stage of its development with formation of Λ-structures (see the scheme in Fig. 9). A secondary high-frequency disturbance generated in the region of origination of streaky structures [Kozlov, 2002] leads to destruction of azimuthal spikes from the vortex ring, thus, intensifying mixing of the jet with the ambient gas and its turbulization. The high-frequency disturbance is developed on two counter rotating vor-

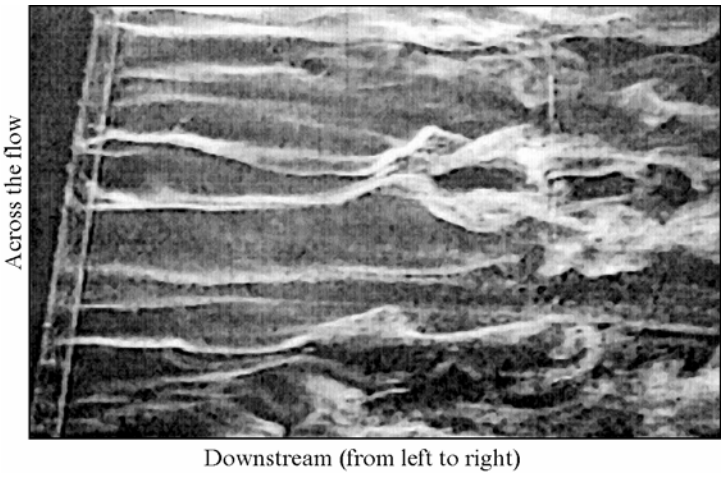

Fig. 6. Visualization of streaky structures in a turbulent boundary layer ((D. Bogart, S. Trujilo) from [Panton, 2001]).

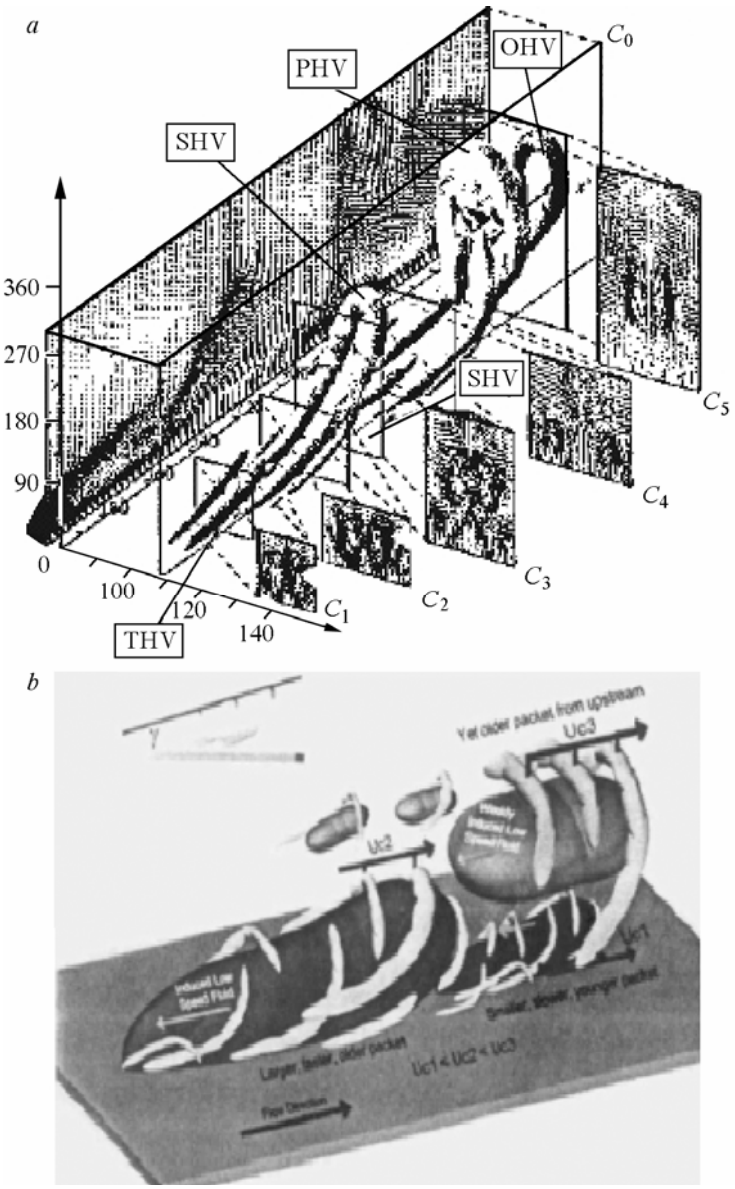

Fig. 7. Vortex structures of a turbulent flow in a channel —numerical experiment (from [Zhou, 1999]) (*a*) and packets of hairpin vortices in a viscous sublayer of a turbulent boundary layer (from [Adrian, 2000]) (*b*).

tices, constituents of Λ - or Ω-shaped azimuthal spikes whose instability to such disturbances was demonstrated in [Grek, 2000]. Thus, the streaky structures play an important role not only in near-wall transitional and turbulent flows but also in free shear flows, such as circular and plane jets. The mechanisms of their origination, development, and interaction with other disturbances, as well as the role in the processes of turbulization and regeneration of turbulence are considered in detail by many researchers.

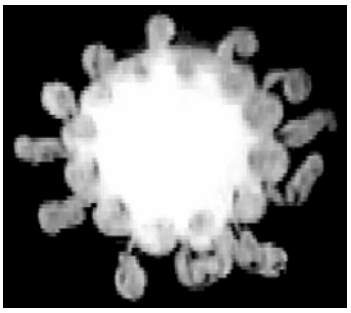

Fig. 8. Visualization of the cross section of a circular jet in the course of interaction of an annular vortex with streaky structures and formation of azimuthal Λ-structures (from [Kozlov, 2002] and [Litvinenko, Kozlov, 2004]).

The high-frequency secondary instability of transitional and turbulent flows with streaky structures is often associated with the so-called sinusoidal and varicose instability. For instance, visualization of the flow modulated by Goertler vortices [Floryan, 1991; Bippes, 1972; Ito, 1985] (see Figs. 2 and 3) showed that the transition in such a flow is determined by secondary mechanisms, which produce instability waves independent on each vortex pair so that the neighboring pairs can amplify different types of secondary motion: either in the form of periodic "meandering" of vortices in the transverse direction or in the form of horse-shoe bunches in the region of a strong transverse shear (Fig. 10).

Such disturbances are called the sinusoidal and varicose mode, respectively. They are compared by many researchers with the odd and even modes known from the analytical and numerical analysis of secondary instability of Goertler vortices. The reason

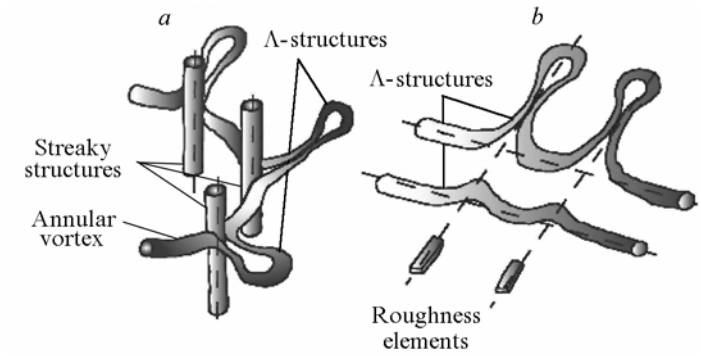

Fig. 9. Scheme of three-dimensional distortion of a two-dimensional annular vortex on local inhomogeneities of the flow (streaky structures) (*a*) and two-dimensional instability wave on roughness elements (*b*) (from [Litvinenko, Kozlov, 2004]).

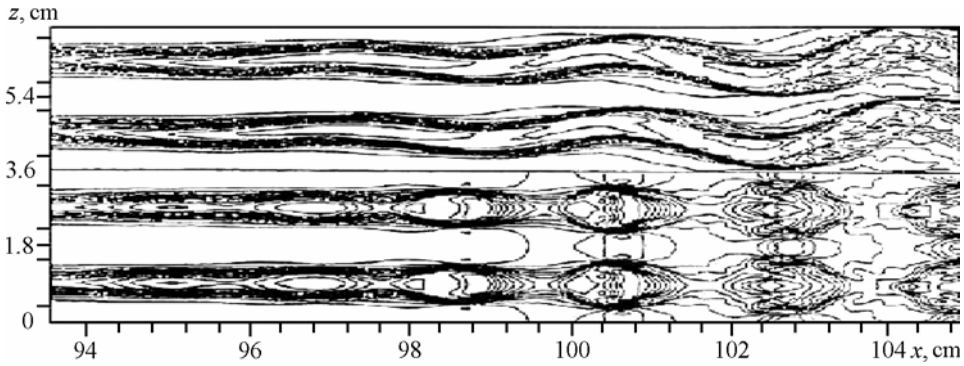

Fig. 10. Distribution of instantaneous velocities in the *xz* plane, the upper and lower figures show the sinusoidal and varicose modes (from [Li, 1995]).

for instability is the inviscid local mechanism caused by inflections in instantaneous velocity profiles both in the normal (varicose mode) and in the transverse (sinusoidal mode) directions. The choice of the instability mode excited first and growing most rapidly depends on particular initial conditions, in particular, on the distance between the disturbances. For instance, it was found numerically [Li, 1995; Bottaro, 1996] that the varicose mode dominates in long-wave vortices, whereas the sinusoidal mode prevails in short-wave vortices, which are more frequently encountered. The reason is that vortices with a long wavelength initiate a weak transverse shear, and vortices with a small wavelength initiate a large shear. Direct numerical simulation of varicose instability in a turbulent boundary layer [Skote, 2002] revealed that horse-shoe vortices generated in the laminar and turbulent boundary layers are similar. It was found simultaneously that the mechanism of generation of horse-shoe vortices in turbulent boundary layers is related to inflectional ($\partial U/\partial y$) instability of streaky structures. Horse-shoe vortices can be the reason for appearance of new streaky structures in the viscous sublayer of the turbulent boundary layer, which agrees with the results of [Adrian, 2000]. On the other hand, sinusoidal instability associated with the transverse inflectional profile of velocity ($\partial U/\partial z$) has been confirmed in many studies [Waleffe, 1977; Kawahara, 1998; Schoppa, 1997]. We can assume that both types of instability are important mechanisms of turbulence self-sustaining in the turbulent boundary layer: the sinusoidal type serves to regenerate near-wall turbulence [Jimenez, 1991; Hamilton, 1995; Brandt, 2002], and the varicose type serves to generate horse-shoe vortices occupying the region farther from the wall [Acarlar, 1987; Haidary, 1994; Adrian, 2000; Skote, 2002; Robinson, 1991]. Results of direct numerical simulation of the sinusoidal and varicose modes of instability of the streaky structure are shown in Figs. 11 and 12 [Skote, 2002; Brandt, 2002].

Instability of a three-dimensional shear layer associated with near-wall streaky structures was studied experimentally in the boundary layer on a flat plate in [Robinson, 1991]. A symmetric (varicose) and an antisymmetric (sinusoidal) modes were excited separately on a single streaky structure (Fig. 13).

Both instability modes were examined under controlled conditions at the linear and initial stages of nonlinear evolution of the laminar-turbulent transition. When the transverse size of the streaky structure was greater than the shear-layer thickness, varicose instability growth was observed. On the other hand, when the transverse size of the streaky structure was commensurable with the shear-layer thickness or smaller than the

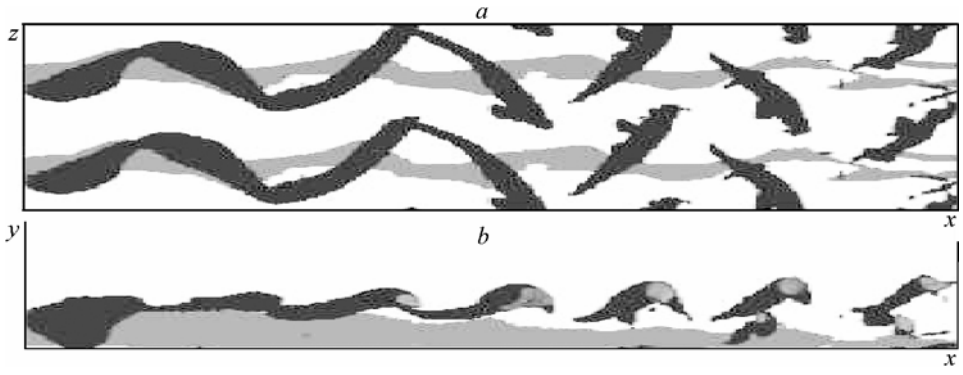

Fig. 11. Numerical experiment on sinusoidal instability of streaky structures in a turbulent boundary layer.

In the plane *xz* (*a*), in the plane *xy* (from [Brandt, 2002]) (*b*).

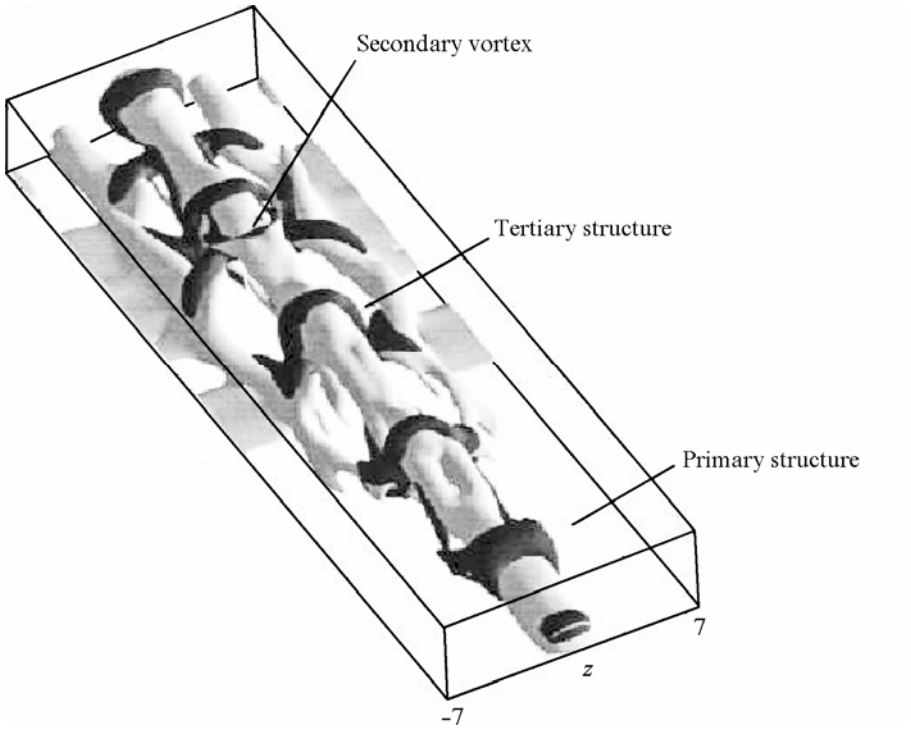

Fig. 12. Numerical experiment on varicose instability of the streaky structure: formation of Ω-vortices is visible (from [Skote, 2002]).

latter, the structure became more unstable with respect to antisymmetric modes rather than to symmetric ones. The experiment [Asai, 2002] clearly demonstrated that the growth of the symmetric mode leads to formation of hairpin vortices, which are a pair of counterrotating streamwise vortices coupled by a head, i. e., a Λ-vortex, whereas the antisymmetric mode is developed into a wave train of quasi-streamwise vortices with vorticity of alternating sign. The study of varicose instability of a single streaky structure in the boundary layer on a swept wing [Asai, 2002] showed that, in contrast to the experiment [Litvinenko, 2004], Λ-vortices are transformed into asymmetric structure because of the influence of the crossflow (Figs. 14 and 15).

The sinusoidal instability of a group of streaky structures responsible for generation of quasi-streamwise vortices in the near-wall region of a turbulent boundary layer was experimentally studied in [Konishi, 2004]. It was found that the development of subharmonic modes does not depend much on the transverse step of streaky structures, whereas the growth of fundamental modes strongly depends on the latter and is completely suppressed when the transverse step becomes 2.5 times smaller than the width of a separate streak.

The present review is aimed at considering the results of recent studies dealing with the development of disturbances in various shear flows and, on the basis of the analysis of these works, presenting the results of our experimental investigations of the nonlinear stage of varicose and sinusoidal instability of the streaky structure in the Blasius boundary layer. The main attention was paid to coherent structures arising in the course of secondary high-frequency instability of streaky structures of the varicose and sinusoidal types, which is important for understanding mechanisms

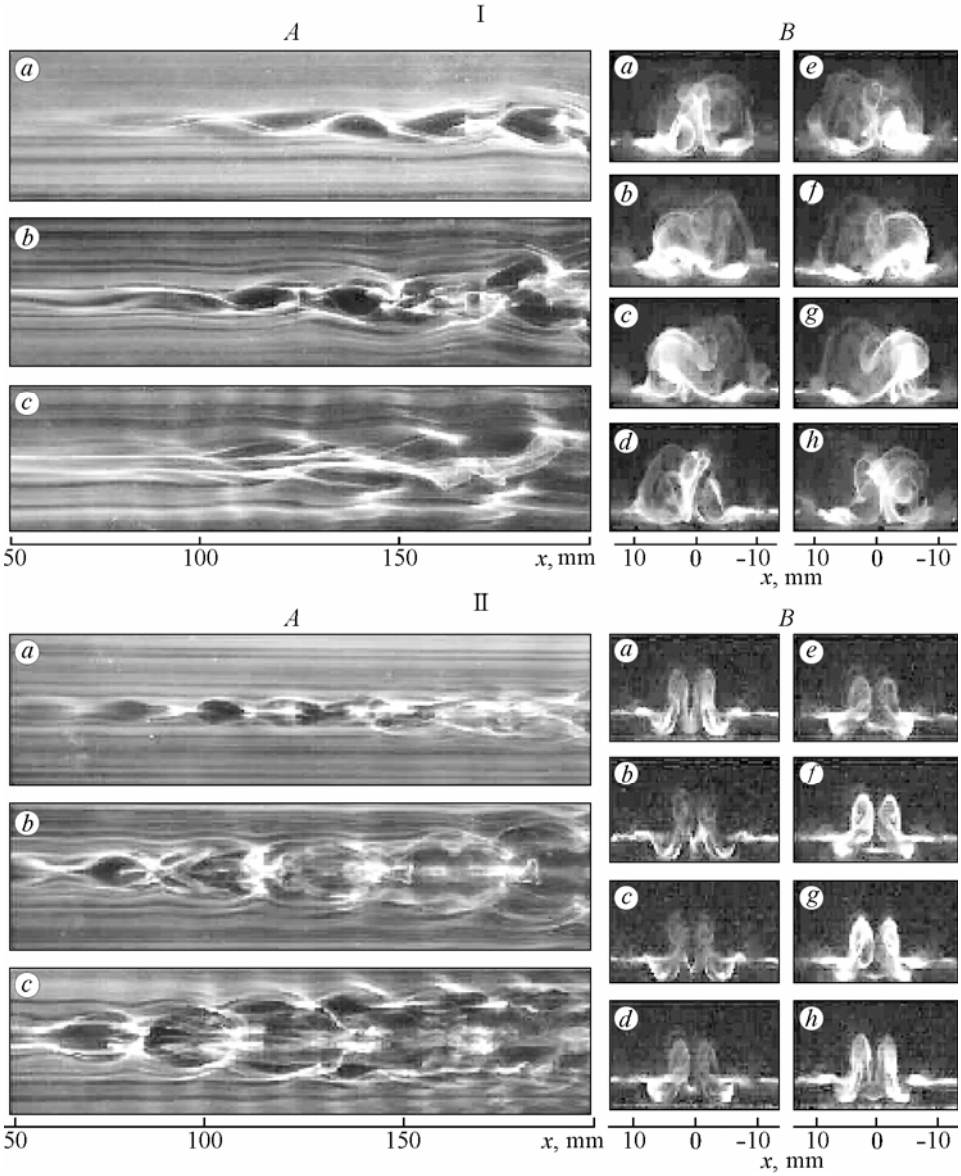

Fig. 13. Visualization of the sinusoidal (I) and varicose (II) instability of the streaky structure in the streamwise direction (*A*) for y = 4, 3, and 2 mm (*a*, *b*, *c*) and in the transverse direction (*B*) with 1/8 of the period (*a*-*h*) (visualization patterns from [Asai, 2002]).

of transition to turbulence and mechanisms of turbulence regeneration in the turbulent boundary layer. In contrast to the experiment [Asai, 2002], the study was performed in more detail (hot-wire measurements of the streamwise velocity and fluctuating velocity over the space (*xyz*) were performed at 5000 points) from the viewpoint of revealing the specific features from origination and development of the internal structure of coherent elements to later stages of their nonlinear development.

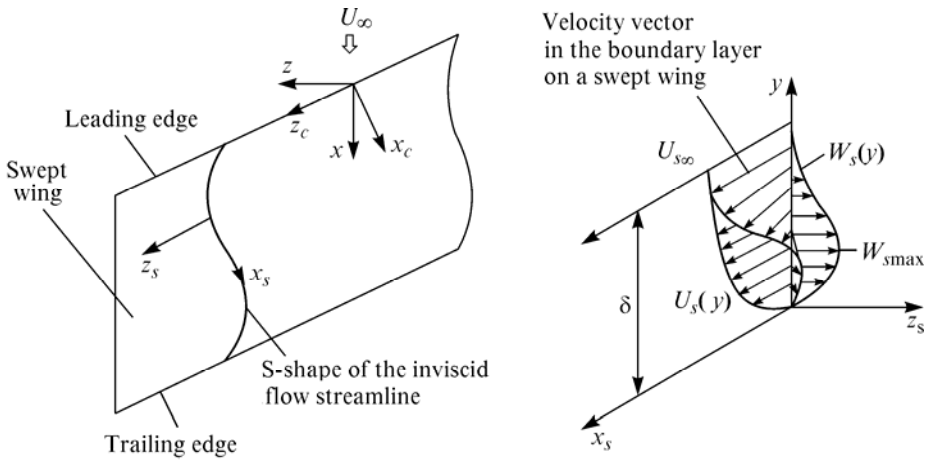

Fig. 14. Velocity components of a three-dimensional boundary layer on a swept wing (from [Litvinenko, 2004]).

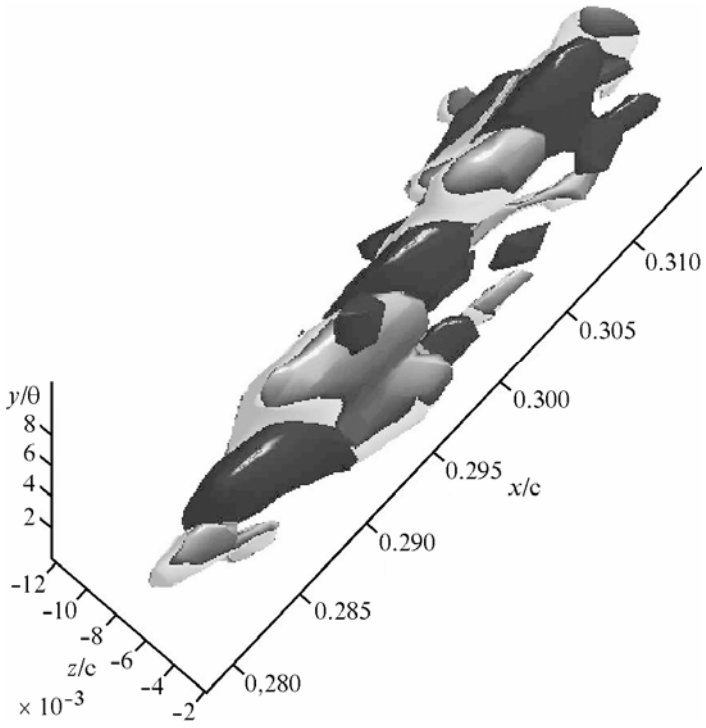

Fig. 15. Spatial pattern of a high-frequency secondary disturbance developed on the streaky structure in the boundary layer on a swept wing (from [Litvinenko, 2004]).

1. EXPERIMENTAL SETUP AND MEASUREMENT PROCEDURE

The experiment was performed in a subsonic low-turbulent wind tunnel on a flat plate (Fig. 16) mounted in the test section. The flow velocity was U_∞ = 7.8 m/s, and the level of turbulence was within 0.1 % for U_∞ = 5–15 m/s in the frequency range from 0.5 to 10,000 Hz.

The plate had an elliptic tip with the axes ratio of 12:1. The streaky structure was generated by a cylindrical roughness element 1.1 mm high and 5.8 mm in diameter; this element was placed in the center of the flat plate at a distance of 438 mm from the tip. The coordinate axes were directed downstream (x), normal to the surface (y), and in the transverse direction (z); the position of the roughness element x = 438 mm is marked by x_0.

In the absence of the roughness element, the laminar boundary layer was developed without any waves, and the velocity profile was close to the Blasius profile. The height of the roughness element h = 1.1 mm is close to the laminar boundary-layer displacement thickness δ_B^* = 1.5 mm for $x = x_0$ and U_∞ = 7.8 m/s. The Reynolds number was $\mathrm{Re}^* = \delta_B^* \cdot U_\infty/\nu$ = 572 for $x = x_0$. The streaky structure made the velocity profile inflectional; they were approximated by a hyperbolic-tangential function in the normal-to-wall direction (y) and by wake-type profiles in the transverse direction (z), as will be demonstrated below.

Without introduction of artificial disturbances, the boundary layer with the streaky structure remained laminar in the measurement region $x - x_0$ = 30–150 mm. This allowed us to control the instability of the streaky structure with the help of artificial disturbances through three orifices 3 mm in diameter. One orifice (z = 0) at $x - x_0$ = 14.5 mm was used to excite transverse symmetric disturbances, and two other orifices were used to excite antisymmetric disturbances $\Delta z = \pm 4.5$ mm at $x - x_0$ = 19.5 mm. Three orifices were separately connected to three loudspeakers by vinyl tubes. The antisymmetric disturbances were excited by sinusoidal signals in antiphase. The excited frequency of the secondary high-frequency disturbance was 150 Hz, which approximately corresponded to the di-

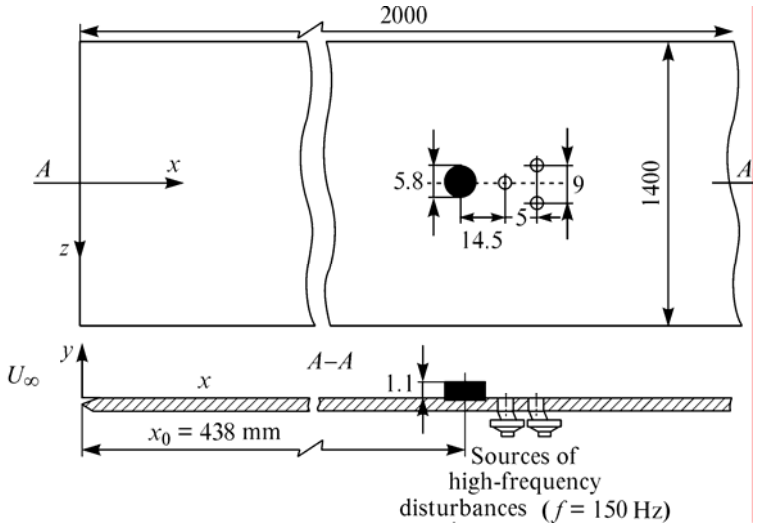

Fig. 16. Layout of the experiment.

mensionless frequency parameter $2\pi f\nu/U_\infty^2 \times 10^6$ = 232. The amplitude of the secon-

dary disturbance reached 10 % U_∞ near the source ($x - x_0$ = 30 mm), which allowed us to study the nonlinear stage of the process of greatest interest to us. The hot-wire anemometer measured the time-averaged streamwise component of velocity U and velocity fluctuations u'. The hot-wire probe with a gilded tungsten wire 1 mm long and 5 μm in diameter, with an overheating coefficient of 1.8, was calibrated in the free stream with the use of the modified King's law $U = k_1\left(E^2 - E_0^2\right)^{1/n} + k_2(E - E_0)^{1/2}$, where E and E_0 are the output voltages of the hot-wire anemometer at the flow velocity and in its absence, respectively, k_1, k_2, and n are constants. The exponent (n) is normally close to 0.5, and the second constant (k_2) takes into account free convection on the wall at low velocities of the flow. The maximum error in probe calibration was within 1 % U_∞. All measurements were performed in an automatic regime with the use of a coordinate gear moving the probe in the space (xyz) by a specially developed program involving LabVIEW. The measurement process included recording of ensemble-averaged oscillograms (up to 50 samples) at a certain spatial point into the computer memory, after which the probe was automatically moved to the next point, etc. The information obtained was processed by the MatLab software, which allowed us to present measurement results in the form of contour diagrams of isolines of mean velocity and velocity oscillations in transverse sections (plane yz) of disturbance development and in the form of space-time (in the coordinates x, y, z, t) patterns of the process.

2. VELOCITY FIELD DOWNSTREAM OF THE ROUGHNESS ELEMENT

Figures 17, *a* and 17, *b* show the distributions of the mean velocity U over y and z at $x - x_0$ = 30 mm. The value of $U = f(y)$ was measured at z = 0 mm and is compared with the velocity distribution at z = –7 mm, where the Blasius profile is outside the zone of influence of the roughness element. The profile of $U = f(y)$ at z = 0 mm behind the roughness element has a clear inflection point, which indicates its instability. In Fig. 17, *b,* the z-distributions are measured at heights y = 1.9, 2.3, 3.1, 3.9, and 4.3 mm. The velocity defect because of deceleration by the roughness element is observed further downstream: y = 4 mm. The transverse distributions of velocity across the streaky structure resemble the distributions in a usual wake; hence, the transverse scale of the streaky structure is marked as half of the width l_s used for conventional wakes. Here, half of l_s is approximately 4 mm for $x - x_0$ = 30 mm. In addition, note that the velocity excess at the end faces of the step, embedded by streamwise vortices (two legs of the horse-shoe vortex arising in the flow around the roughness element) is significantly greater than that in [Asai, 2002] because of the influence of the secondary disturbance. This indicates that the action of the steady horse-shoe vortex with a superposed secondary disturbance on the velocity field is significantly greater than that in the same paper [Asai, 2002]. The present streaky structure is not, therefore, free from streamwise vorticity because of the presence of artificial disturbances. The presence of inflection points in the profiles *U(z)* indicates their instability, as is the case with the profile $U(y)$.

The contour diagrams of isolines of equal defects of mean velocity in the plane yz near the roughness element at x_0 = 30 mm under conditions of generation of secondary high-frequency disturbances exciting the sinusoidal (*a*) and varicose (*b*) types of instability are shown in Fig. 18. In both cases, the structure of the flow field shown by mean velocity isolines is the region of the velocity defect and two regions of velocity excess located symmetrically about the velocity-defect region. This is a typical flow structure in the form of isolines for two counterrotating vortices, which in this case are "legs" of the hairpin vortex generated by the flow around the roughness element.

The secondary disturbance of velocity exerted a noticeable effect on the intensity of mean flow characteristics, which is associated with the nonlinearity of this process already

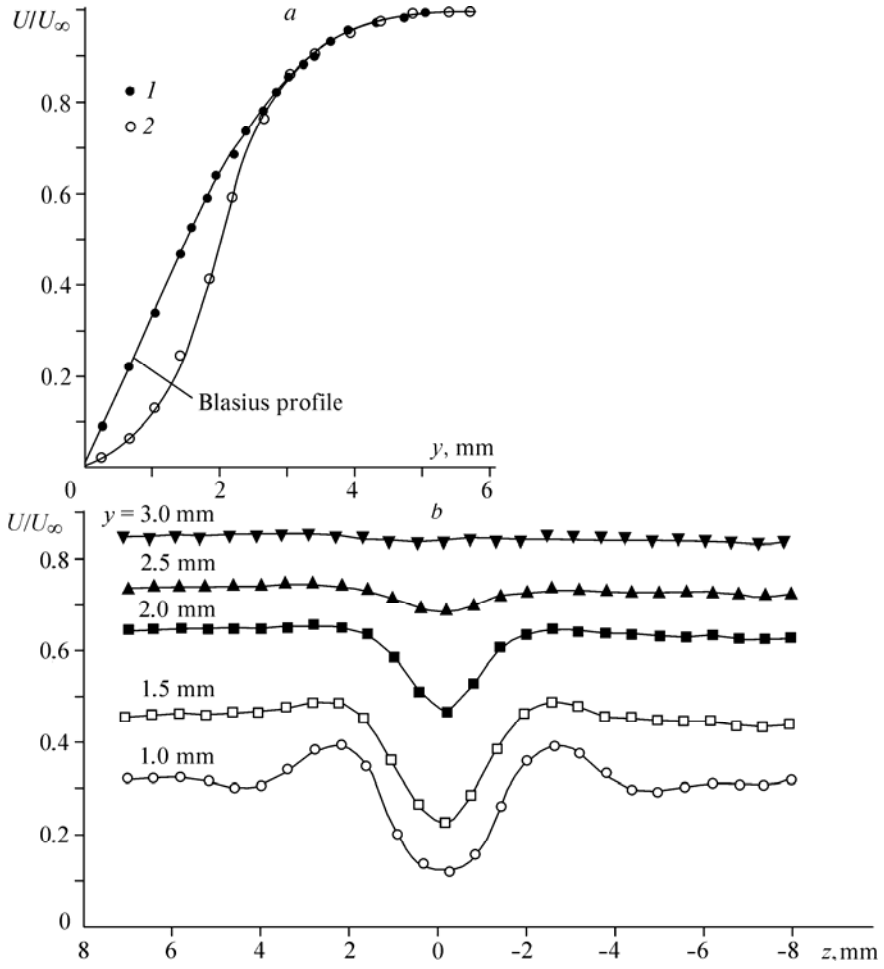

Fig. 17. *y*- and *z*-distributions of the mean velocity U for $x - x_0 = 30$ mm.

a —*y*-distributions for z = 0 (*1*); 7 mm (*2*); *b* —*z*-distributions of the mean velocity at different distances from the wall.

near the source of disturbances. The maximum amplitude of mean velocity reaches 17 % U_∞ for varicose instability and 23 % U_∞ for the sinusoidal type. A weak shift of the maximum in the velocity-defect distribution upward from the wall can be observed in Fig. 18, *b*, which seems to be related to the action of the disturbance immediately ahead of the streaky structure in the case of varicose instability. The contour diagrams of isolines of equal velocity fluctuations (u'_{RMS}) in Fig. 19 give an idea about the structure of the secondary high-frequency disturbance of the sinusoidal and varicose types near the roughness element in the plane *yz* at $x - x_0 = 30$ mm.

As is seen from Fig. 19, the amplitude of fluctuations of the secondary disturbance is rather high even near the roughness element, especially for the varicose type of instability: 10.2 % U_∞ (the value for the sinusoidal type is 3.5 % U_∞). Thus, conditions are created for the nonlinear stage of development of both types of instability further downstream. Considering the common properties of instability of inflectional velocity profiles in the *y* and *z* directions, we expected that the streaky structure can grow by two types of the unstable mode, i. e., the symmetric varicose mode developed into symmetric hairpin vortices with a pair of counterrotating streamwise vortices and the antisymmetric sinusoidal mode leading to meandering of the streaky structure. To excite these two instabil-

ity modes separately, the disturbances in the control experiment were inserted into the laminar streaky structure

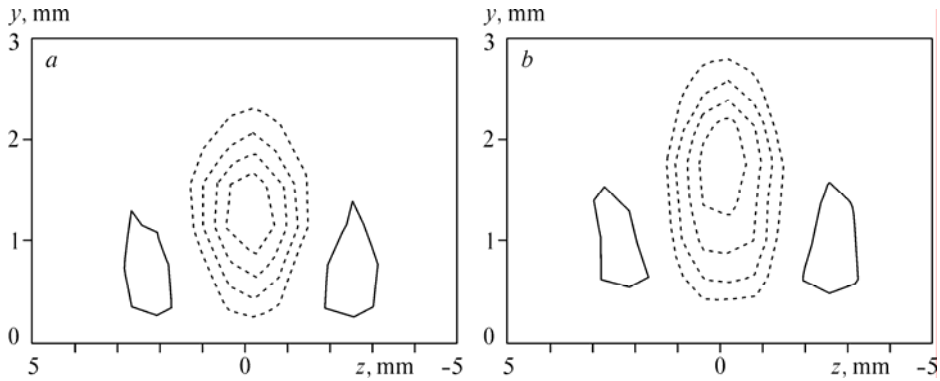

Fig. 18. Contour diagrams of isolines of equal velocity defects in the *yz* plane near the roughness element for $x - x_0 = 30$ mm.

a — sinusoidal instability (amplitudes –16.4 %; –12.6 %; –8.6 %; –4.7 %; 7 % U_∞) and *b* — varicose instability (amplitudes –11.3 %; –8.4 %; –5.6 %; –2.8 %; 5.6 % U_∞).

through small orifices connected to the loudspeaker, as was already noted above. Figure 19, *a* shows the antisymmetric mode with $f = 150$ Hz. The distribution of this mode is symmetric with respect to $z = 0$, but its phase is subjected to a 180-degree jump across the axis of symmetry; thus, the amplitude of this mode disappears at $z = 0$. Figure 19, *b* shows the symmetric mode at the same frequency $f = 150$ Hz, which is close to the mode that is most rapidly growing under natural conditions. The distribution of this mode, vice versa, displays the maximum amplitude at $z = 0$ and the absence of the transverse jump in phase. Thus, the excited waves can be identified as the inherent modes of a three-dimensional shear layer related to the streaky structure. Despite a clearly nonlinear character of the excited waves even near the source of their generation, the distributions in Fig. 19 correlated qualitatively with similar distributions in [Asai, 2002]. Note, the phase velocities of the symmetric and antisymmetric modes were close to the local velocity at inflection points in the profile along the *y* axis at $z = 0$ mm and

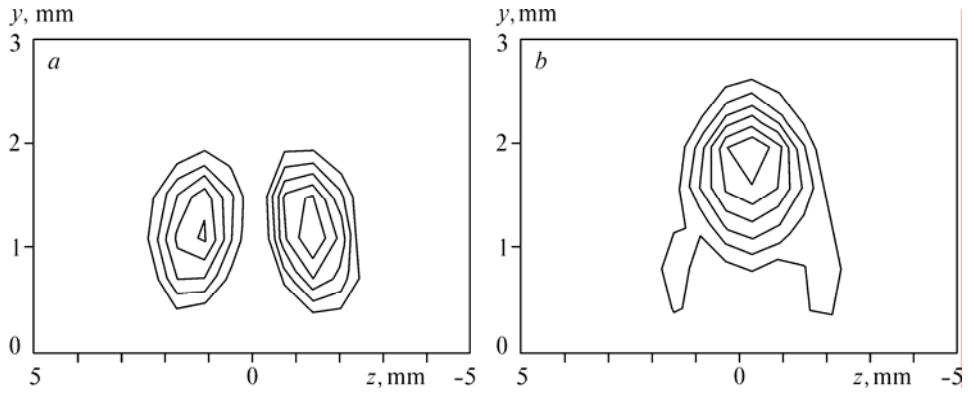

Fig. 19. Contour diagrams of isolines of equal velocity fluctuations of the secondary high-frequency disturbance for the sinusoidal (*a*) and varicose (*b*) types of instability near the roughness element $x - x_0 = 30$ mm.

The step of isolines for u'/U_∞: 1.5 %; 2 %; 2.6 %; 3.1 %; 3.5 % (*a*); 2.9 %; 4.3 %; 5.9 %;7.3 %; 8.7 %; 10.2 % (*b*).

along the z axis at y = 2 mm, respectively. The shift of velocity ($\partial U/\partial y$ or $\partial U/\partial z$) attains the highest value at these inflection points.

3. ORIGINATION OF COHERENT STRUCTURES IN NONLINEAR DEVELOPMENT OF THE SINUSOIDAL AND VARICOSE MODES OF INSTABILITY

It is known [Asai, 2002] that linear instability of a three-dimensional shear layer is related to the streaky structure. It is of interest to consider how instability modes evolve to coherent vortices leading to near-wall turbulence. As was already noted, the amplitude of artificial disturbances responsible for generation of nonlinearity and later stages of transition near the roughness element at $x - x_0$ = 30 mm was 3.5 % U_∞ and 10 % U_∞ for the sinusoidal and varicose instability modes, respectively. The growth rate of high-frequency secondary disturbances in the downstream direction (from $x - x_0$ = 30 mm to $x - x_0$ = 150 mm) was rather weak (from 3.5 % U_∞ to 11 % U_∞ for the sinusoidal mode and from 10 % U_∞ to 12 % U_∞ for the varicose mode), whereas the influence of disturbances on the mean flow characteristics was fairly significant (from 19 % U_∞ to 38 % U_∞ for the sinusoidal instability mode and from 7 % U_∞ to 32 % U_∞ for the varicose mode). The influence of sinusoidal instability is particularly strong: it exerts a powerful effect on the mean flow parameters (38 % U_∞) even if the amplitude of the secondary disturbance is considerably smaller (3.5 % U_∞). This supports the conclusions of many researchers that sinusoidal instability is more dangerous.

Let us compare the evolution of the sinusoidal and varicose instability modes at the nonlinear stage, which was studied in the present work and in [Asai, 2002]. Figure 20 shows the ensemble-averaged contour diagrams of isolines of equal velocities in the xz plane, taken from [Asai, 2002], and the spatial patterns of velocity defects with a superposed secondary disturbance in the (xyz) space from the present work at five uniformly spaced moments of time over the period for the sinusoidal disturbance (see Fig. 20, *a*) and at four uniformly spaced moments of time over the period of the varicose disturbance (see Fig. 20, *b*). The frequencies of the sinusoidal and varicose disturbances in [Asai, 2002] were f = 60 and 110 Hz, respectively; the frequency in the present work was f = 150 Hz. At the initial stage of development of the sinusoidal disturbance ($x \approx$ 60–70 mm), one can see meandering of the streaky structure over the half-period by 180° in these works (see Fig. 20, *a*). Further downstream, however, multiplication of streaky structures, appearance of coherent structures such as Λ-vortices in Fig. 20, *a*, II and the absence of such dynamics in Fig. 20, *a*, I. A similar picture is also observed in the case of development of varicose instability (see Fig. 20, *b*). The initial stage of spatial development in these works reflects periodic pinching of the streaky structure, but further downstream the hot-wire measurements reveal multiplication of streaky structures and emergence of coherent structures (see Fig. 20, *b*, II), whereas such a phenomenon was not observed in [Asai, 2002] (see Fig. 20, *b*, I). We can assume that the nonlinear stage of development of both types of instability in [Asai, 2002] was examined only at the initial stage of the process and with less detailed hot-wire measurements than those used in the present study.

Let us consider the flow structure behind the roughness at the nonlinear stage of sinusoidal and varicose instability in more detail. Figure 21 shows the sinusoidal destruct

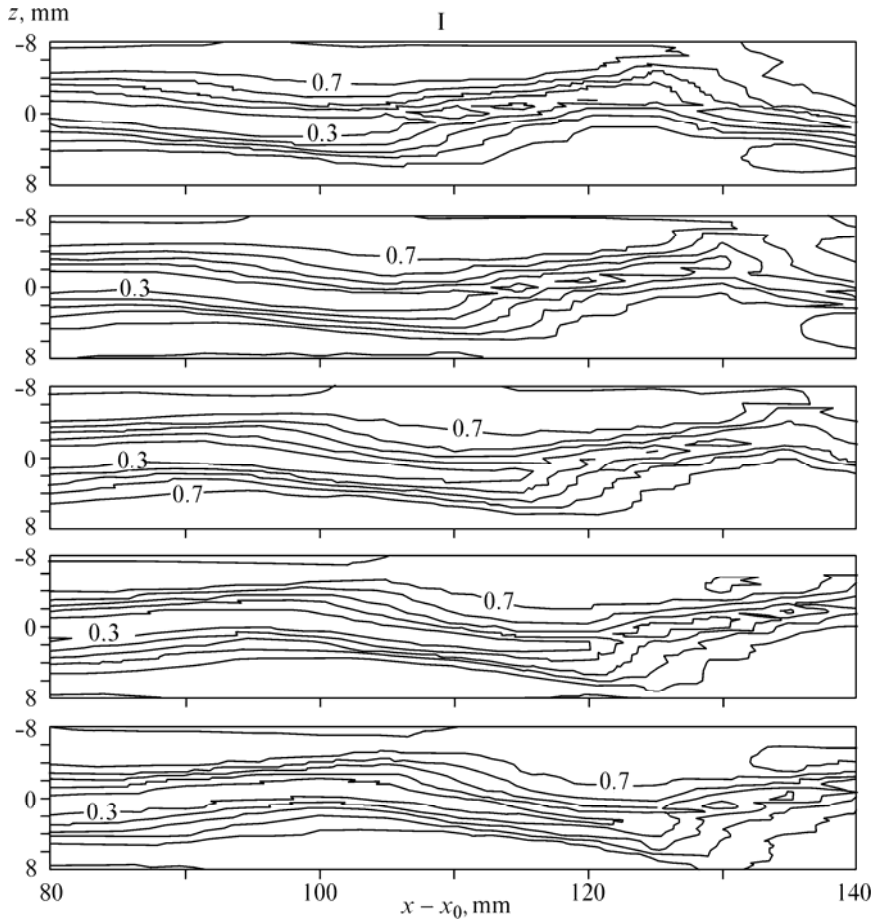

Fig. 20a. Ensemble-averaged contour diagrams of isolines of equal velocity in the case of excitation of the sinusoidal mode in the *xz* plane at y = 3 mm from [Asai, 2002] (I) and spatial patterns of development of the sinusoidal mode in the (*xyz*) space from the present work (II). The time intervals over the period t/T = 0 (*a*), 1/8 (*b*), 2/8 (*c*), 3/8 (*d*), 4/8 (*e*).

tion of the streaky structure. The contour diagrams of isolines of equal velocity defects together with the disturbance in the *yz* plane (Fig. 21, II) demonstrate transverse smearing of the disturbed flow region in the downstream direction, which is associated with multiplication of streaky structures (generation of new streaky structures). This is evidenced by the appearance of new closed regions of isolines at $x - x_0$ = 150 mm. The spatial pattern of the disturbance (Fig. 21, I) shows that meandering of the streaky structure in the transverse direction is observed at the initial part of the flow, which is typical of the development of sinusoidal instability. Further downstream, however, the structure of the disturbed region is transformed into typical coherent structures, which resemble Λ-vortices. Let us consider the development of the secondary high-frequency disturbance generated on the streaky structure. The contour diagrams of isolines of equal velocity fluctuations in the *yz* plane (Fig. 22, II) demonstrate transverse fragmentation of the initially simple structure in the downstream direction into a number of closed regions of isolines near the plate wall (up to seven for $x - x_0$ = 150 mm). The oscillating (meandering) streaky structure leads to generation of a "train" of streamwise vortices entrained downstream, as was found in [Asai, 2002]; apparently, we also observe this process in

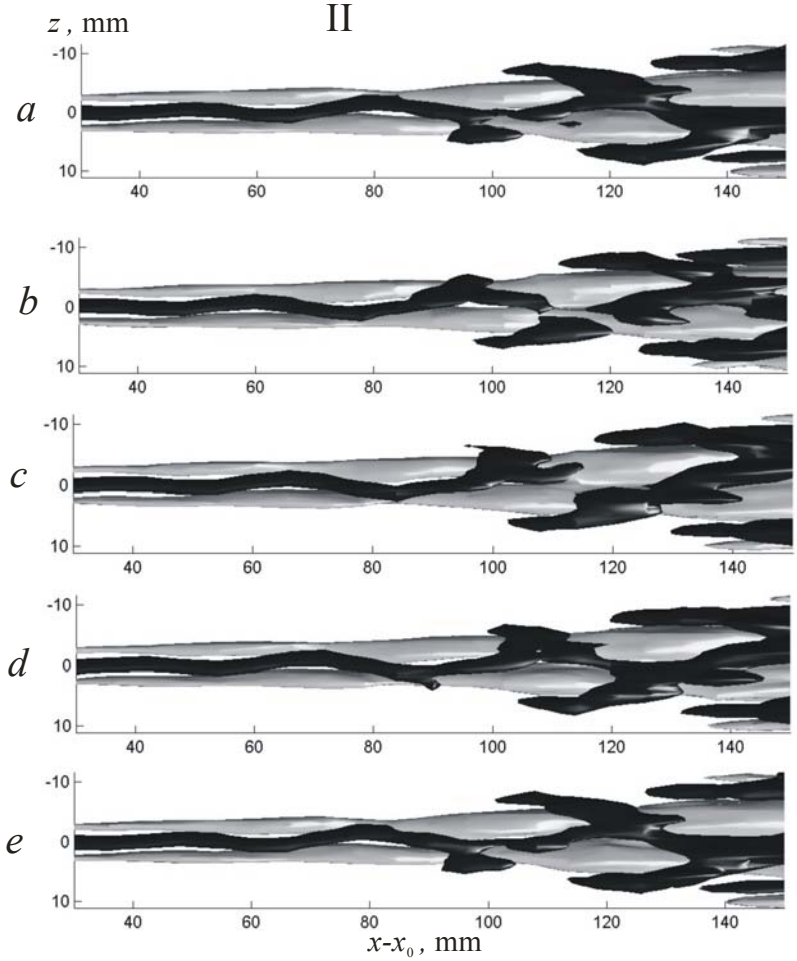

Fig. 20a. Continued.

the present work but with transverse multiplication of these vortices. The process of development of secondary disturbances is particularly well observed in the spatial pattern in Fig. 22, I. At the initial stage of disturbance evolution, we can observe a pair of quasi-streamwise vortices of alternating sign, which are transformed further downstream into Λ-structures; the transverse scale of these coherent structures increases thereby. It should be noted that appearance of coherent structures such as quasi-streamwise vortices but not Λ–structures were observed in [Asai, 2002] in studying the nonlinear stage of sinusoidal instability. A possible reason is a less detailed consideration of the disturbed region and consideration of only initial stages of the nonlinear process. In a less detailed consideration of the disturbed flow pattern with the level of disturbance amplitude of 6.4 % U_∞ (Fig. 23, III), we can mainly observe structures such as quasi-streamwise vortices, whereas in the case of the spatial pattern with the disturbance amplitude of 0.4 % U_∞ (see Fig. 23, I), one can see typical coherent structures such as Λ-vortices. Thus, detailed hot-wire measurements of the nonlinear stage of sinusoidal instability showed that the secondary high-frequency destruction of the streaky structure is associated with formation of Λ-structures whose downstream evolution leads to flow turbulization.

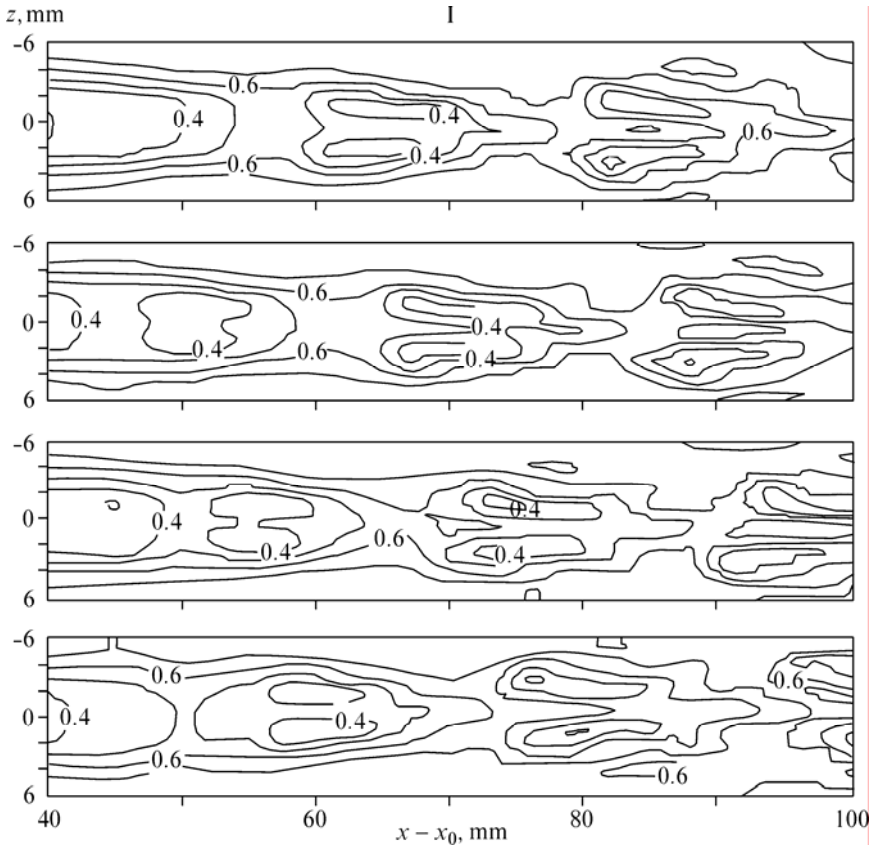

Fig. 20b. Ensemble-averaged contour diagrams of isolines of equal velocity in the case of excitation of the varicose mode in the *xz* plane at $y = 3$ mm from [Asai, 2002] (I) and spatial patterns of development of the sinusoidal mode in the (*xyz*) space from the present work (II). The time intervals over the period $t/T = 0$ (*a*), 1/4 (*b*), 2/4 (*c*), 3/4 (*d*).

Figure 24 shows the patterns of varicose destruction of the streaky structure. The contour diagrams of equal velocity defects together with the disturbance in the *yz* plane (Fig. 24, II) demonstrate transverse smearing of the disturbed region in the downstream direction, which is related to multiplication of streaky structures (generation of new streaky structures). This is evidenced by emergence of new closed regions of isolines at $x - x_0 = 72$ and 108 mm. The spatial pattern of disturbance evolution (Fig. 24, I) shows that streamwise modulation of the streaky structure by the secondary-disturbance frequency ($f = 150$ Hz) is observed at the initial part, which is typical of the development of varicose instability. Further downstream, however, the structure of the disturbed region is transformed into typical coherent structures resembling Λ-vortices, as in the case of sinusoidal destruction of the streaky structure. It should be noted, nevertheless, that, in contrast to the previous case, the Λ-structures are asymmetric, i. e., the second counter-rotating vortex is at the stage of formation because of weak vorticity at transverse boundaries of the disturbance field. Below, in considering the development of the high-frequency disturbance, we will observe symmetric Λ-structures.

Let us consider the development of the secondary high-frequency disturbance generated on the streaky structure. The contour diagrams of isolines of equal velocity oscillations in the *yz* plane (Fig. 25, II) demonstrate transverse fragmentation of the initially simple structure in the downstream direction into a series of closed regions, as in the case with sinusoidal instability. Streamwise modulation of the streaky structure leads to

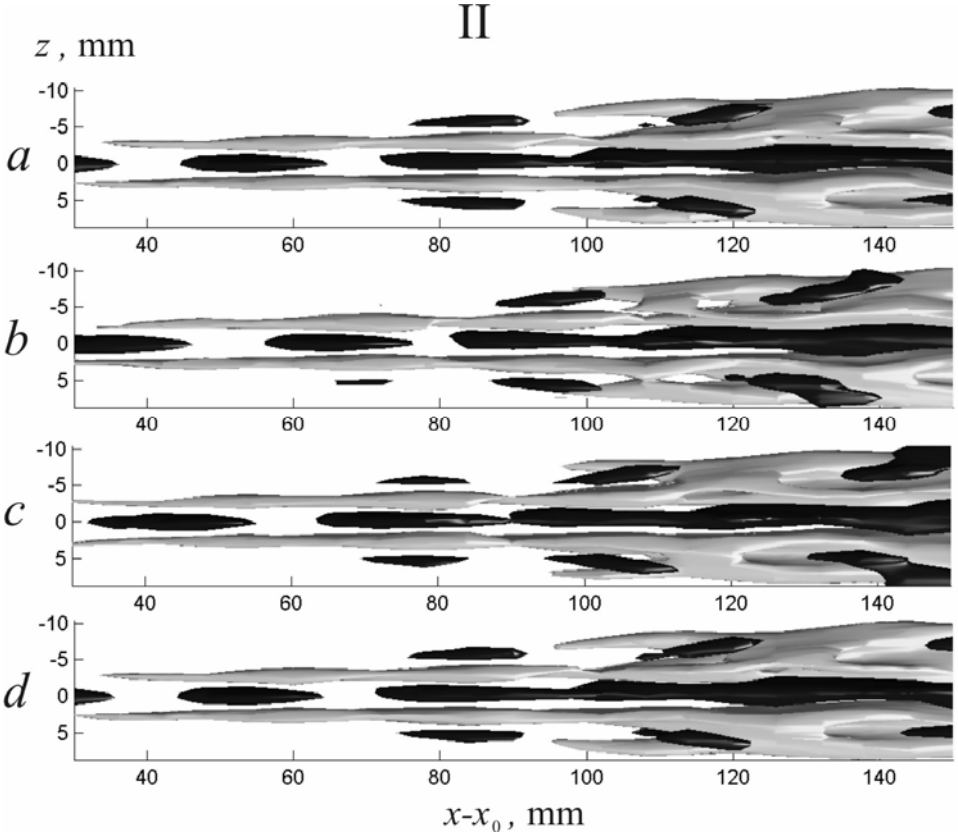

Fig. 20b. Continued.

generation of hairpin vortices or a pair of counterrotating quasi-streamwise vortices in the region $z = \pm 2.5$ mm, as was found in [Asai, 2002]. In our case, apparently, we observe the same process but with transverse multiplication of these vortices. In addition, we can observe upward motion of the low-velocity fluid; each leg of the hairpin vortex evolves into a pair of counterrotating streamwise vortices in x-positions downstream. The process of development of secondary disturbances is particularly well seen in the spatial picture in Fig. 25, I. At the initial stage of disturbance development, we can observe a sequence of quasi-streamwise vortices, which are transformed further downstream into hairpin vortices or Λ-vortices. These vortices are clearly seen at $z = 0$ mm in the form of a pair of structures of alternating sign in each period of the secondary disturbance. At $z = \pm 5$ mm, the transverse boundaries of the disturbed region, the Λ-structures or hairpin vortices become asymmetric, as was noted above; nevertheless, the structure of the second counterrotating vortex of these coherent structures is clearly observed. It should be noted that exactly such coherent structures were observed in [Asai, 2002] in studying the nonlinear stage of varicose instability. On the other hand, asymmetric Λ-structures were found in the development of the varicose mode of flow instability in the boundary layer ona swept wing [Litvinenko, 2004] (see Fig. 15). Simultaneously, transformation of coherent structures of the varicose instability mode into structures of sinusoidal instability because of the crossflow on a swept wing was observed in [Litvinenko, 2004].

Let us consider the spatial pattern of development of the secondary high-frequency disturbance in the form of surfaces of equal levels of amplitude for 2.6 % U_e, 1.4 % U_e

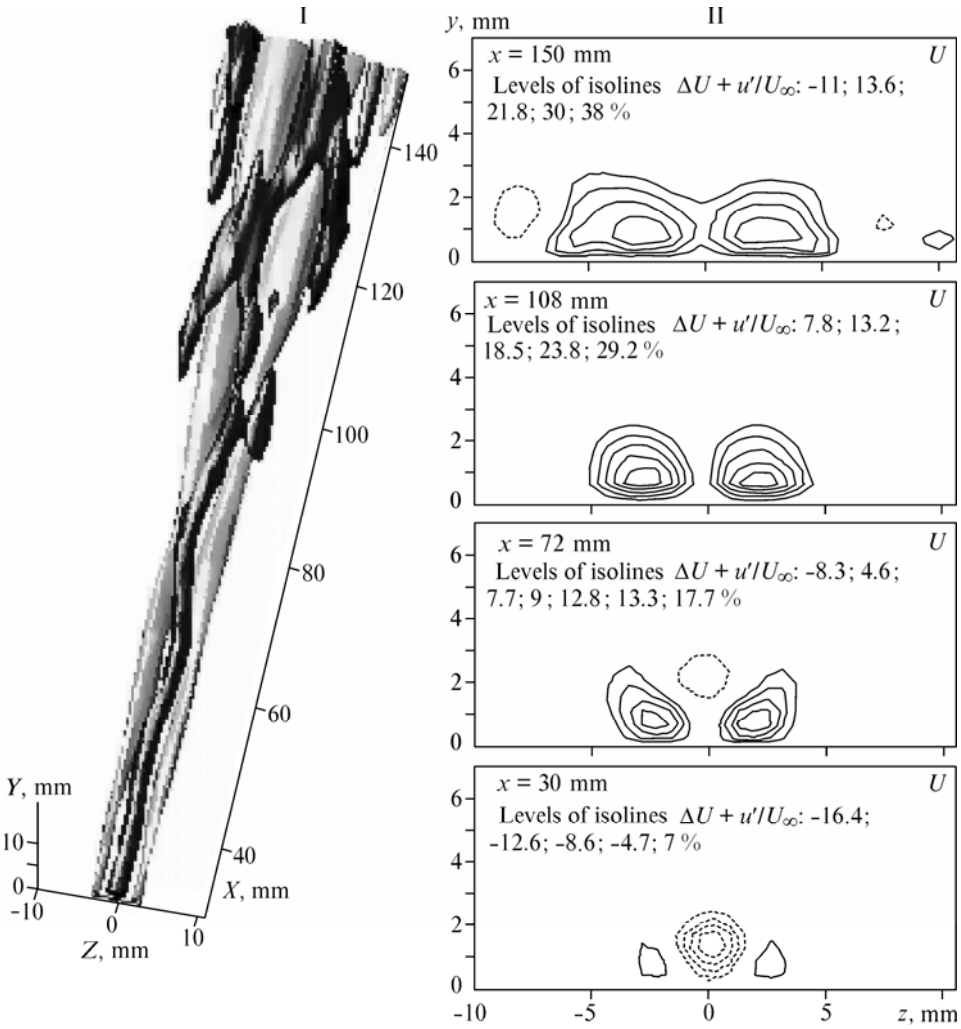

Fig. 21. Patterns of sinusoidal destruction of the streaky structure: spatial pattern of disturbance evolution together with its influence on the mean velocity (the minimum level of fluctuations is 6.4 % U_∞, the dark and light shadows indicate the velocity excess and defect, respectively) (I), contour diagrams of isolines of equal defects of the mean velocity in the plane *yz* at different distances in the downstream direction (the solid and dashed isolines refer to the velocity excess and defect, respectively) (II).

and 0.4 % U_∞ (Fig. 26). In a less detailed consideration of the flow pattern in the disturbed region, e.g., in the case of the spatial pattern at the level of disturbance amplitude of 2.6 % U_∞ (see Fig. 26, III), we can observe localized vortices of streamwise modulation of the streaky structure at the initial stage of disturbance development. Further downstream, there follows the process of transverse multiplication of structures and emergence of Λ-vortices. In considering the flow pattern in the disturbed region at the level of disturbance amplitude of 0.4 % U_∞ (see Fig. 26, I), we can see origination of Λ-vortices at a significantly earlier stage of the disturbance. Thus, detailed hot-wire measurements of the nonlinear stage of development of the varicose instability mode

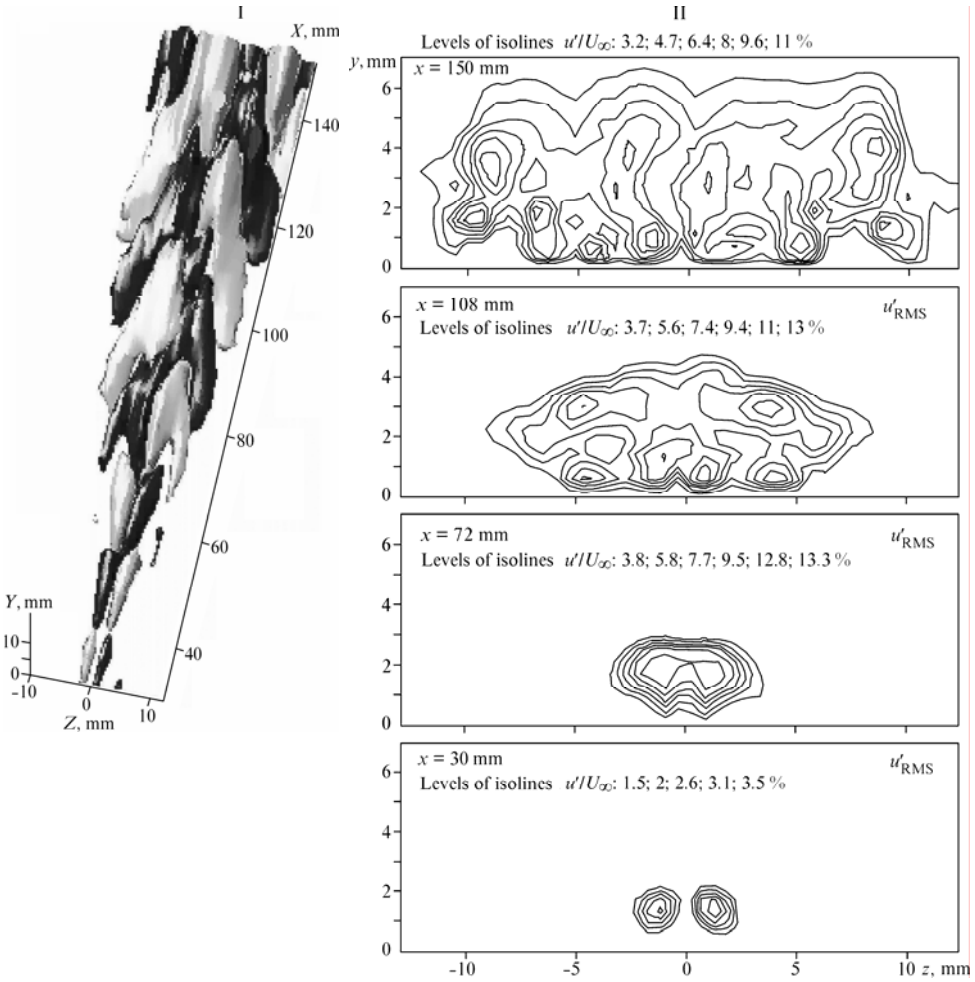

Fig. 22. Patterns of sinusoidal destruction of the streaky structure: spatial pattern of disturbance evolution (the minimum level of fluctuations is 1.3 % U_∞, the dark and light shadows indicate the velocity excess and defect, respectively) (I), contour diagrams of isolines of equal root-mean-square fluctuations of velocity in the plane *yz* at different distances in the downstream direction (II).

showed that secondary high-frequency destruction of the streaky structure, as in the case of sinusoidal destruction, is related to formation of Λ-structures.

Finally, we should note that the scenario of the classical laminar-turbulent transition at the nonlinear stage of this process is associated with three-dimensional distortion of the two-dimensional Tollmien — Schlichting waves and formation of three-dimensional coherent structures such as Λ-vortices. The present investigations showed that there are other scenarios of origination of Λ-structures in near-wall shear flows, in particular, in the process of secondary high-frequency instability of streaky structures of the sinusoidal and varicose types. This result is important both for understanding the mechanism of turbulization of flows modulated by streaky structures and for understanding the mechanisms of turbulence reproduction in turbulent flows, where the dynamics of coherent structures of the viscous sublayer plays an important role. On the other hand,

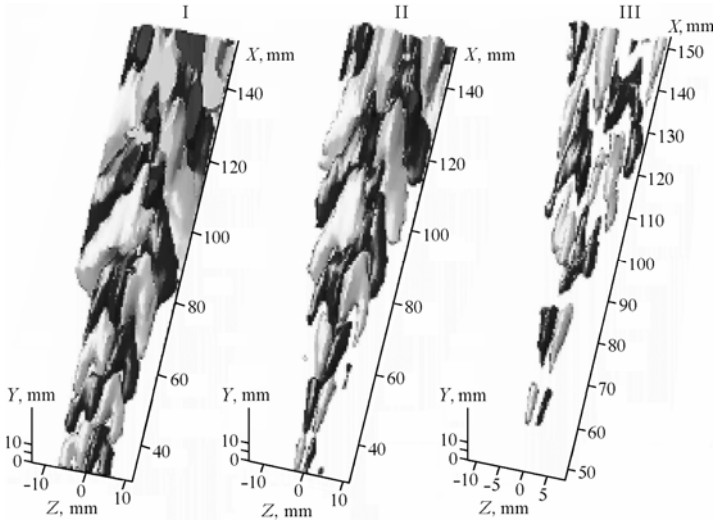

Fig. 23. Spatial patterns of development of the secondary high-frequency disturbance of the nonlinear stage of sinusoidal instability.

Surfaces of equal levels of amplitude —0.4 % (I); 1.3 % (II), 6.4 % U_∞ (III) (the dark and light shadows indicate the velocity excess and defect, respectively).

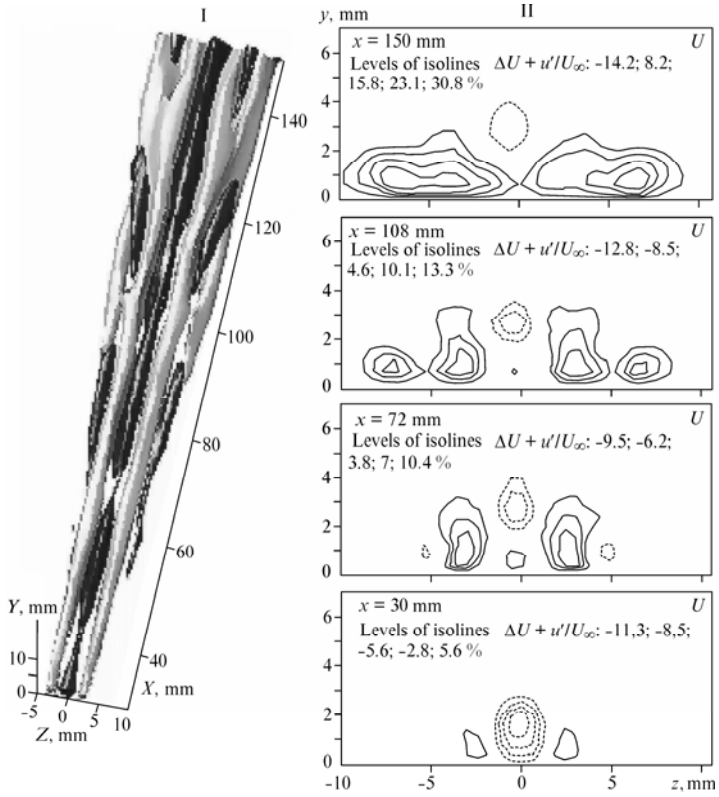

Fig. 24. Patterns of varicose destruction of the streaky structure.

Spatial pattern of disturbance evolution together with its influence on the mean velocity (the minimum level of fluctuations is 3.8 % U_∞, the dark and light shadows indicate the velocity excess and defect, respectively) (I), contour diagrams of isolines of equal defects of the mean velocity in the *yz* plane at different distances in the downstream direction (the solid and dashed isolines refer to the velocity excess and defect, respectively) (II).

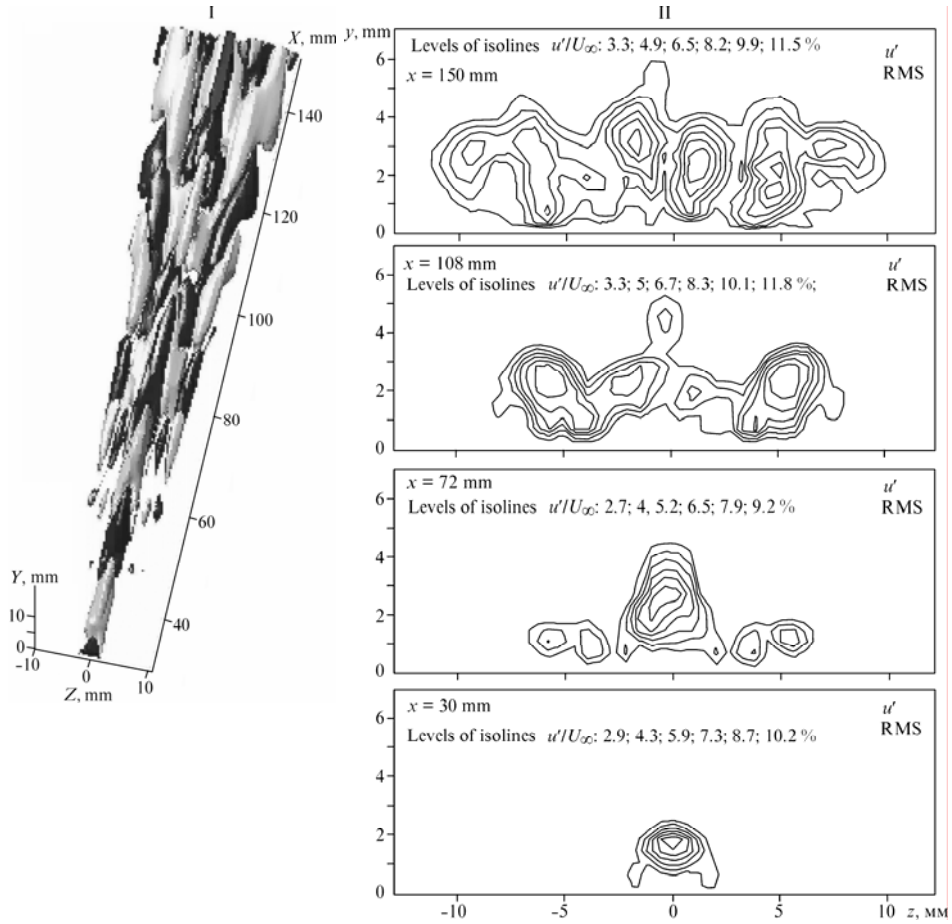

Fig. 25. Patterns of varicose destruction of the streaky structure.

Spatial pattern of disturbance evolution (the minimum level of fluctuations is 1.3 % U_∞, the dark and light shadows indicate the velocity excess and defect, respectively) (I), contour diagrams of isolines of equal root-mean-square fluctuations of velocity in the plane *yz* at different distances in the downstream direction (II).

various methods are known for controlling the development of coherent structures such as Λ-vortices, hairpin vortices, streaky structures, etc. It was shown in some papers that riblets, localized and distributed suction, transverse oscillations of the wall, etc. exert a significant effect on intensity of coherent structures, which can be used to control both sinusoidal and varicose instability modes.

5. CONCLUSIONS

In addition to formation of Λ–structures at the nonlinear stage of the laminar-turbulent transition in the boundary layer with rollup of the two-dimensional wave, there may exist nonlinear mechanisms of sinusoidal and varicose modes of instability of streamwise streaky structures. On the basis of experimental investigations of this stage of both instability modes, we can draw the following conclusions.

1. Secondary high-frequency instability of the streaky structure of the sinusoidal and varicose types at the nonlinear stage leads to multiplication of new streaky structures in the downstream direction.

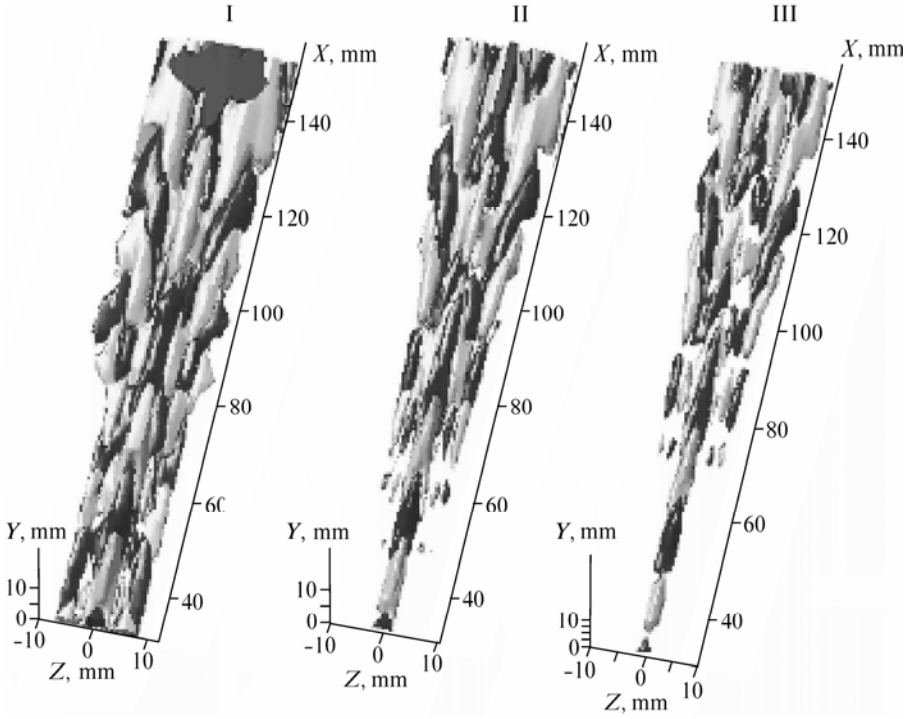

Fig. 26. Spatial patterns of development of the high-frequency disturbance of the nonlinear stage of varicose instability.

Surfaces of equal levels of amplitude —0.4 % (I); 1.3 % (II), 2.6 % U_∞ (III) (the dark and light shadows indicate the velocity excess and defect, respectively).

2. The mechanism of nonlinear destruction of the streaky structure by means of development of the secondary disturbance is related to formation of coherent structures such as Λ-vortices for both sinusoidal and varicose modes of instability.

3. It is shown that Λ-vortices multiply in the transverse direction in the course of downstream evolution of the disturbance.

4. Varicose instability can exist on a swept wing, rapidly transforming under the action of the secondary mean flow to a superposition of sinusoidal and varicose instability modes.

REFERENCES

Y.S. Kachanov, V.V. Kozlov, and V.Ya. Levchenko, Origination of Turbulence in the Boundary Layer (in Russian), Nauka, Novosibirsk, 1982, 151 p.

V.V. Kozlov, G.R. Grek, L.L. Loefdahl, V.G. Chernorai, and M.V. Litvinenko, Role of streamwise localized structures in the transition to turbulence in boundary layers and jets (review), J. Appl. Mech. Tech. Phys., 2002, Vol. 43, No. 2, P. 62-76.

M.V. Litvinenko, V.V. Kozlov, G.V. Kozlov, and G.R. Grek, Effect of streamwise streaky structures on turbulization of a circular jet, J. Appl. Mech. Tech. Phys., 2004, Vol. 45, No. 3, P. 50-61.

Yu.A. Litvinenko, G.R. Grek, V.V. Kozlov, L. Loefdahl, and V.G. Chernorai, Experimental study of varicose instability of the streaky structure in the boundary layer on a swept wing, Thermophys. Aeromech., 2004, Vol. 11, No. 1, P. 1-10.

M.S. Acarlar and C.R. Smith, A study of hairpin vortices in a laminar boundary layer. Pt 1, J. Fluid Mech., 1987, Vol. 175, P. 1-41.

R.J. Adrian, C.D. Meinhart, and C.D. Tomkins, Vortex organization in the outer region of the turbulent boundary layer, J. Fluid Mech., 2000, Vol. 422, P. 1-23.

M. Asai, M. Minagawa, and M. Nishioka, The stability and breakdown of near-wall low-speed streak, J. Fluid Mech., 2002, Vol. 455, P. 289–314.

H. Bippes, Experimentelle Untersuchung des laminar-turbulenten Umschlags an einer parallel angestroemten konkaven Wand, Sitzungsberichte der Heidelberger Akademie der Wissenschaften Mathematisch-naturwissenschaftliche Klasse, Jahrgang 1972, 3 Abhand-lung, P. 103–180. (also NASA-TM-72243, March 1978).

A.V. Boiko, G.R. Grek, A.V. Dovgal, and V.V. Kozlov, The Origin of Turbulence in Near-Wall Flows, Springer Verlag, Berlin et al., 2002, P. 1–263.

A. Bottaro and B.G.B. Klingmann, On the linear breakdown of Goertler vortices, Europ. J. Mech. B/Fluids, 1996, Vol. 15, No. 3, P. 301–330.

L. Brandt and D.S. Heningsson, Transition of streamwise streaks in zero-pressure-gradient boundary layers, J. Fluid Mech., 2002, Vol. 472, P. 229–261.

J.M. Floryan, On the Goertler Instability of Boundary Layers: Technical Report of National Aerospace Laboratory, TR-1120, 1991, P. 1-45.

G.R. Grek, V.V. Kozlov, M.M. Katasonov, and V.G. Chernorai, Experimental study of a Λ-structure and its transformation into the turbulent spot, Current Sci., 2000, Vol. 79, No. 6, P. 781–789.

H.A. Haidary and C.R. Smith, The generation and regeneration of single hairpin vortices, J. Fluid Mech., 1994., Vol. 227, P. 135–151.

H. Hamilton, J. Kim, and F. Waleffe, Regeneration of near-wall turbulence structures, J. Fluid Mech., 1995, Vol. 287, P. 317.

A. Ito, Breakdown structure of longitudinal vortices along a concave wall, J. Japan Soc. Aero. Space Sci., 1985, Vol. 33, P. 166–173.

J. Jimenez and P. Moin, The minimal flow unit in near-wall turbulence, J. Fluid Mech., 1991, Vol. 225, P. 213–226.

Y.S. Kachanov, On a universal mechanism of turbulence production in wall shear flows, Notes on Numerical Fluid Mechanics and Multidisciplinary Design. Vol. 86. Recent Results in Laminar-Turbulent Transition., Springer Verlag, Berlin et al., 2003, P. 1–12.

G. Kawahara, J. Jimenez, M. Uhlmann, and A. Pinelli, The instability of streaks in near-wall turbulence: Center for Turbulence Research, Annual Research Briefs, 1998, P. 155–170.

P.S. Klebanoff, K.D. Tidstrom, and L.M. Sargent, The three-dimensional nature of boundary-layer instability, J. Fluid Mech., 1962, Vol. 12, P. 1–34.

Y. Konishi and M. Asai, Experimental investigation of the instability of spanwise-periodic low-speed streaks in a laminar boundary layer, Japan Fluid Mech. J., 2004, No. 02–1257, P. 55-67.

F. Li and M.R. Malik, Fundamental and subharmonic secondary instabilities of Goertler vortices, J. Fluid Mech., 1995, Vol. 82, P. 255-290.

R.L. Panton, Overview of the self-sustaining mechanisms of wall turbulence, Progress in Aerospace Sci., 2001, No. 37, P. 341–383.

P.R. Pratt, V.G. Chernoray, A.A. Bakchinov, and L. Loefdahl, A quantitative flow visualization of a point source disturbance in a swept wing boundary layer, Boundary Layer Transition in Aerodynamics: Book of abstracts EUROMECH Colloquium 423, Stuttgart, 2001.

J. Reuter and D. Rempfer, A hybrid spectral/finite-difference scheme for the simulation of pipe-flow transition, Laminar-Turbulent Transition, H. Fasel, W.S. Saric (eds.), Springer Verlag, Berlin et al., 2000, P. 383–390.

U. Rist, K. Moeller, and S. Wagner, Visualization of late-stage transitional structures in numerical data using vortex identification and feature extraction, Proc. 8th Intern. Symp. Flow Visualization. Sorrento, 1998, Pap. No. 103.

S.K. Robinson, The kinematics of turbulent boundary layer structure: NASA TM 103859, 1991.

W.S. Saric, V.V. Kozlov, and V.Ya. Levchenko, Forced and unforced subharmonic resonance in boundary layer transition, AIAA Pap. 84-0007, 1984.

W. Schoppa and F. Hussain, Genesis and dynamics of coherent structures in near-wall turbulence: A new look, Self-sustaining Mechanisms of Wall Turbulence, R.L. Panton (ed.), Computational mechanics, Southampton, 1997.

M. Skote, J.H. Haritonidis, and D.S. Henningson, Varicose instabilities in turbulent boundary layers, Physics of Fluids, 2002, Vol. 4, No. 7, P. 2309-2323.

F. Waleffe, On a self-sustaining process in shear flows, Phys. Fluids, 1997, Vol. 9, P. 883-896.

J. Zhou, R.J. Adrian, S. Balachandar, and T.M. Kendal, Mechanisms for generating coherent packets of hairpin vortices in channel flow, J. Fluid Mech., 1999, Vol. 387, P. 353–396.